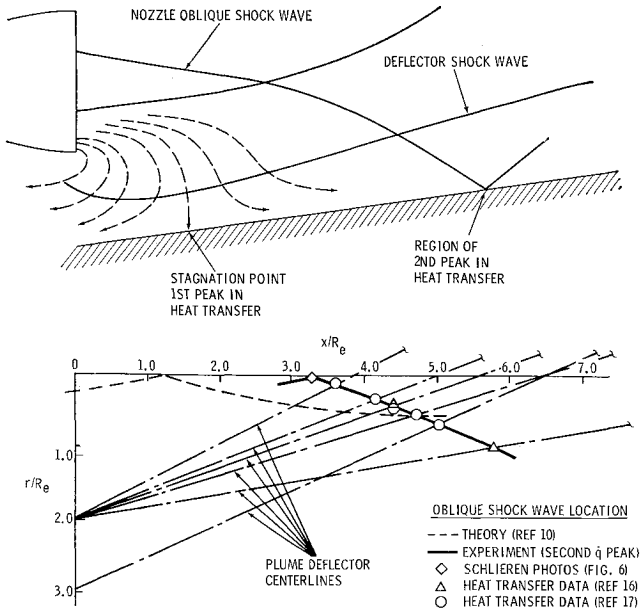

Fig. 8 Sketch of flow along plume deflector centerline and scale drawing of nozzle oblique shock wave location inferred from second $\dot{q}$ peaks on plume deflector centerlines ($\frac{1}{4}$-scale LM RCS nozzle).

in the far field may give very misleading results when applied to near-field problems.

References

[1] Leng, J., Oman, R. A., and Hopkins, H. B., "A Detonation Tube Technique for Simulating Rocket Plumes in a Space Environment," *Journal of Spacecraft and Rockets*, Vol. 5, No. 10, Oct. 1968, pp. 1148–1154.

[2] Stitt, L. E. and Latto, W. T., "Highly Underexpanded Exhaust Jets Against Adjacent Surfaces," *Astronautics and Aerospace Engineering*, Vol. 1, No. 1, Feb. 1963, pp. 107–110.

[3] Back, L. H. and Cuffel, R. F., "Detection of Oblique Shocks in a Conical Nozzle with a Circular-Arc Throat," *AIAA Journal*, Vol. 4, No. 12, Dec. 1966, pp. 2219–2221.

[4] Eastman, D. W. and Radtke, L. P., "Flow Field of an Exhaust Plume Impinging on a Simulated Lunar Surface," *AIAA Journal*, Vol. 1, No. 6, June 1963, pp. 1430–1431.

[5] Andrews, E. H., Vick, A. R., and Craidon, C. B., "Theoretical Boundaries and Internal Characteristics of Exhaust Plumes from Three Different Supersonic Nozzles," TN D-2650, March 1965, NASA.

[6] Roberts, L., "The Interaction of a Rocket Exhaust with the Lunar Surface," *The Fluid Dynamic Aspects of Space Flight*, AGARDograph 87, Vol. 2, Gordon and Breach, New York, 1966, pp. 269–290.

[7] Piesik, E. T., Koppang, R. R., and Simkin, D. J., "Rocket-Exhaust Impingement on a Flat Plate at High Vacuum," *Journal of Spacecraft and Rockets*, Vol. 3, No. 11, Nov. 1966, pp. 1650–1657.

[8] Herron, R. D., "Jet-Boundary Simulation Parameters for Underexpanded Jets in a Quiescent Atmosphere," *Journal of Spacecraft and Rockets*, Vol. 5, No. 10, Oct. 1968, pp. 1155–1160.

[9] Brook, J. W., "Far Field Approximation for a Nozzle Exhausting into a Vacuum," *Journal of Spacecraft and Rockets*, Vol. 6, No. 5, May 1969, pp. 626–628.

[10] Rochelle, W. C., *LM RCS Plume Impingement Study*, Rept. 68.3352.16–26, Dec. 1968, TRW Systems, Redondo Beach, Calif.

[11] Nelson, T., Rice, R., and Rosenstock, J., *Results of the First Series of $\frac{1}{20}$-Scale Shock Tube Fire-Till-Touchdown Tests*, LM Engineering Memo LMO-510-984, Oct. 1968, Grumman Aerospace Corp., Bethpage, N.Y.

[12] Clark, L. V., *LM Base Pressures and Retro Nozzle Choking During Simulated Lunar Touchdown*, LWP-632, July 1968, NASA.

[13] Snedeker, R. S. and Donaldson, C. duP., *Experiments on Free and Impinging Underexpanded Jets from a Convergent Nozzle*, Rept. 63, Sept. 1964, Aeronautical Research Associates of Princeton.

[14] Adamson, T. C., Jr. and Nicholls, J. A., "On the Structure of Jets from Highly Underexpanded Nozzles Into Still Air," *Journal of the Aerospace Sciences*, Vol. 26, No. 1, Jan. 1959, pp. 16–24.

[15] Rosenstock, J., Nelson, T., and Rice, R., *Results of the Third Series of $\frac{1}{20}$-Scale Shock Tube Fire-Till-Touchdown Tests*, LM Engineering Memo LMO-510-1093, Feb. 1969, Grumman Aerospace Corp., Bethpage, N.Y.

[16] Osonitsch, C., *Analysis of Shock Tunnel RCS Plume Deflector Pressure and Heat Transfer Data*, LM Engineering Memo LMO-510-1060, Jan. 1969, Grumman Aerospace Corp., Bethpage, N.Y.

[17] Mendelsohn, A. R. and Holland, C., *The LM-A Plume Deflector Aerothermodynamics Analysis and Shock Tunnel Test*, AAP/LM-A Rept. ARP251-6, March 1969, Grumman Aerospace Corp., Bethpage, N.Y.

Projectile Size and Density Effects on Hypervelocity Penetration

R. J. Arenz, S.J.*

Loyola University of Los Angeles, Los Angeles, Calif.

Nomenclature

D = diameter of hole in shield or first sheet, in.
d = diameter of projectile, in.
P = depth of penetration of single target sheet, in.
P_T = total depth of penetration of shield and backup sheet, in.
S = sheet spacing, in.
t = thickness of sheet, in.; t_b for backup sheet; t_s for shield or first sheet; t_∞ for single sheet required for quasi-infinite response
t_T* = "ballistic limit" = value of $(t_s + t_b)/d$ to resist mechanical failure on the inner surface
V = velocity of impact, km/sec
ρ = density of projectile material, g/cm^3

Introduction

THE current generation of spacecraft has incorporated meteoroid shielding appropriate for relatively short-term near-earth and cislunar missions. As planning turns to long duration space stations and interplanetary vehicles, designs must take into account the larger particles expected to be encountered on such extended missions and approaches to the asteroid belt. The NASA Manned Spacecraft Center recently sponsored an experimental test program at the light gas gun facility of the Douglas Aerophysics Laboratory.[1] It examined the penetration characteristics against dual-sheet structures of both low-density syntactic foam and aluminum spheres varying in diameter from 0.125 to 1.22 in. These results have been augmented with data from small aluminum projectiles fired at the NASA/MSC Meteroid Simulation Laboratory, and the scaling effects from both test series are reported here.

Presented as Paper 69-376 at the AIAA Hypervelocity Impact Conference, Cincinnati, Ohio, April 30–May 2, 1969; submitted April 30, 1969; revision received August 27, 1969. This work was sponsored by the NASA Manned Spacecraft Center, Houston, Texas, under a NASA-ASEE Summer Faculty Research Fellowship. It is a pleasure to acknowledge the suggestion of this research by B. G. Cour-Palais as well as helpful discussions with him and W. E. McAllum at the Manned Spacecraft Center.

* Assistant Professor, Department of Mechanical Engineering. Member AIAA.

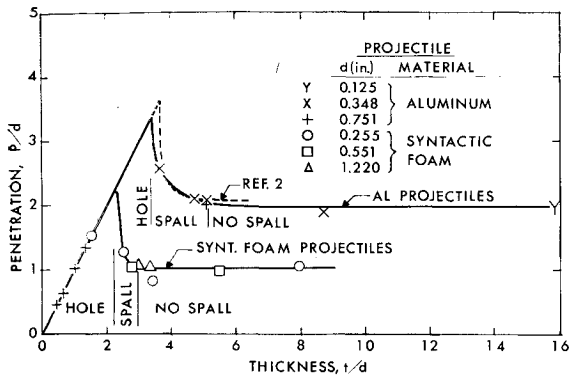

Fig. 1 Normalized depth of penetration in 2024-T3 aluminum single-sheet targets impacted by spherical projectiles; $V \doteq 7.2$ km/sec.

Two projectile materials were used: 2024-T3 aluminum with a density of 2.78 g/cm³ and syntactic foam having a density of 0.70 g/cm³. The latter material consists of tiny hollow glass spheroids in a plastic matrix. The nominal impact velocity for the tests was 7.2 km/sec. All targets were of 2024-T3 A1; however, with the exception of the smaller size sheets used in the MSC tests, they were in the stress-relieved condition, designated 2024-T351, which has essentially similar mechanical properties to T3.

For the purposes of this analysis, the term "ballistic limit" will mean the total thickness of the two-sheet structure at which any mechanical failure (such as a small crack) occurs on the rear face of the backup sheet. Thus, a bulge on the rear face is acceptable as long as no structural rupture appears on that surface even though in this case an internal fracture is probably present.

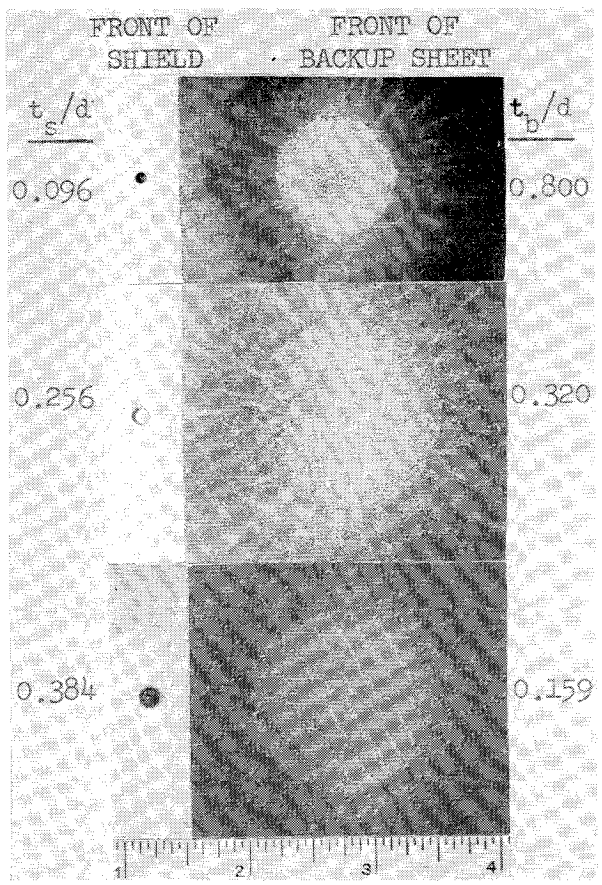

Fig. 2 Effect of shield thickness on hole size in shield and spray pattern on the backup sheet; Al projectiles, $d = 0.063$ in., $V \doteq 7.2$ km/sec; dual-sheet targets, $S/d = 30$.

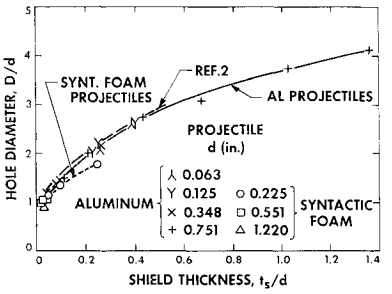

Fig. 3 Hole diameter in Al shields.

Tests with single-sheet targets were made (Fig. 1) to determine whether the larger particle effects correlate with results already available for small size projectiles. The results for aluminum spheres show good agreement with data of Maiden et al.[2] against the same target material; P/d for quasi-infinite (no spalling) targets is 1.96. For the syntactic foam projectiles the quasi-infinite target value is $P/d = 1.01$.

Results for Dual-Sheet Configurations

The pictures in Fig. 2 show the hole diameter in the shield increasing with shield thickness. Results for all the test combinations are plotted in Fig. 3. The curve for the aluminum projectile holes is slightly lower but generally similar to the following empirical relationship of Ref. 2:

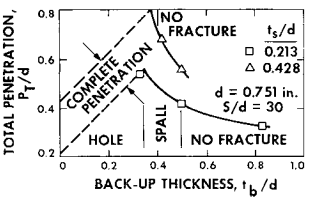

Fig. 4 Total depth of penetration by Al spheres in dual-sheet targets.

$$D/d = 0.45V(t_s/d)^{2/3} + 0.90 \qquad (1)$$

However, evaluation of this expression for the larger particles would produce a growing deviation from the experimental results in which the exponent of t_s/d is slightly less than $\frac{1}{2}$ for the larger values. For the less dense syntactic foam, this exponent is smaller, approximately 0.25.

Figure 2 also illustrates the effect of varying shield thickness on the nature of debris impact on the backup sheet for a constant projectile size and velocity. The "thin" shield (in this case, $t_s/d = 0.096$) upon impact tends to liquefy (and perhaps vaporize), producing a fine spray of small divergence angle to the backup sheet. The deepest craters are thus near the center of the spray pattern on the front of the backup sheet, and the characteristic rear face damage to the backup is consequently a spall centrally located in the impact region.

In contrast, the "medium" shield ($t_s/d = 0.256$), having a larger hole punched out of it, produces a more divergent spray and damage pattern on the backup sheet (Fig. 2). Also, since it is thicker, this shield would require more energy (compared to the thin shield) to liquefy; thus, it generally has unmelted debris particles around the edge which produce a

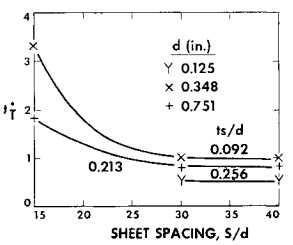

Fig. 5 Ballistic limit vs sheet spacing for dual-sheet targets; Al projectiles.

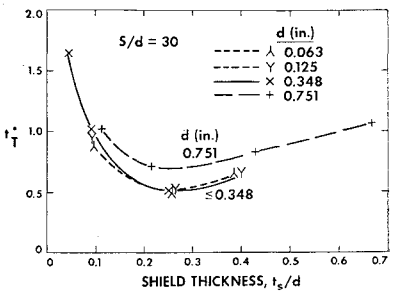

Fig. 6 Ballistic limit vs shield thickness for dual-sheet targets; Al projectiles.

ring of fairly deep craters at the periphery of the spray pattern on the front of the backup sheet. This feature readily distinguishes it from the case of the thin shield. The damage pattern will involve plastic deformation of the central part of the backup if it is thin enough.

Finally, the "thick" shield ($t_s/d = 0.384$) has an even larger hole punched out and often liquefies only slightly so that solid particles of debris from the projectile and shield impact the front of the backup in a wide pattern (as for the medium shield) but in a much more random pattern of deep craters. The rear face of the backup thus typically suffers random spall damage.

The foregoing considerations proved to be of value in determining the ballistic limits for the various structural combinations, particularly for the cases in which hypervelocities were being achieved for the first time in the laboratory for the

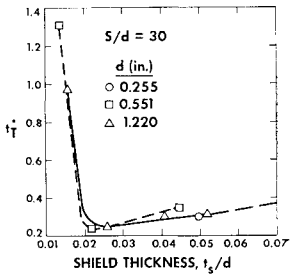

Fig. 7 Ballistic limit vs shield thickness for dual-sheet targets impacted by syntactic foam spheres.

large size projectiles. Because of the associated experimental difficulties, anomolous penetrations and unsymmetrical impact patterns occurred in numerous test specimens. The knowledge of the standard damage pattern in a particular case was used in conjunction with working plots of normalized total penetration p_T/d to aid in determining the ballistic limit. Figure 4 illustrates such a working plot for two sets of test points for the 0.751-in. aluminum projectiles.

These total penetration curves take on characteristic shapes dependent on the parameters t_s/d and S/d, with the ballistic limit occurring in a reasonably narrow region of t_b/d values for a given set of test parameters. From physical reasoning, a continuous variation with t_b/d is expected, so that these plots aid in eliminating possible anomolous test points and in interpolating between test values to establish the ballistic limit with improved accuracy. Most of the ballistic limit values were bracketed by test points so that

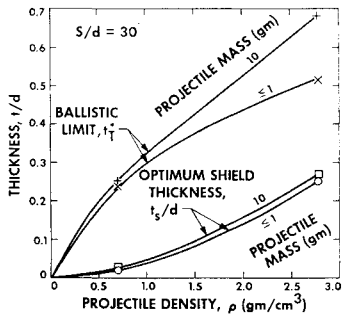

Fig. 8 Variations of t_T^* and corresponding optimum t_S/d with projectile density for 2024-T3 aluminum dual-sheet targets impacted by spherical projectiles; $V \doteq 7.2$ km/sec.

negligible extrapolation was necessary. Nevertheless, a certain amount of scatter remains in the data; the accuracy of ballistic limit determinations is estimated to be within $\pm 5\%$.

Figure 5 indicates a rapid decrease in ballistic limit t_T^* as the sheet spacing ratio S/d increases from 15 to 30, but very little additional benefit between 30 and 40. For $t_s/d = 0.213$,

$$t_T^* \propto S^{-1.4} \quad (15 \leq S/d \leq 30)$$

which compares with $t_T^* \propto S^{-0.75}$ as reported for some 6061 aluminum targets[3] at a t_s/d of 0.25 and a similar spacing range; since it appears that nothing is to be gained by $S/d > 30$, all succeeding comparisons are given for $S/d = 30$.

Figure 6 shows ballistic limit thickness requirements in the neighborhood of optimum shield thickness for aluminum projectiles. The optimum t_s/d is approximately 0.25, and all of the ballistic limits approximately coincide except for the 0.751 in. diam results that are universally higher.

There is more scatter in the syntactic-foam projectile data (Fig. 7) than in the aluminum; possibly this is the result of less regular breakup of this composite material, which may not be completely homogeneous. The optimum t_s/d is 0.025, or $\frac{1}{10}$ the value for the more dense aluminum. The minimum t_T^* is approximately 0.25.

Curves drawn from the origin through the minimum t_T^* values for the two densities give the summary chart (Fig. 8) showing the combined effects of density and mass (size).

A ballistic limit expression given by Nysmith[4] in terms of the velocity of 3.2-mm-diam Pyrex glass particles ($\rho = 2.23$ g/cm^3) is (in the present notation)

$$V_{B.L.} = 0.059(S/d)^2(t_T^*)^{2.5} \qquad (2)$$

For the test velocity of 7.2 km/sec and $S/d = 30$, this estimate (involving a slightly more rigorous ballistic limit damage criterion) would require $t_T^* = 1.13$. Results of the present program would predict $t_T^* = 0.47$, with optimum t_s/d, whereas Nysmith used equally thick shield and backup sheets. Thus, the present results confirm Nysmith's statement that his equation should be conservative.

Conclusions

Experimental results at $V \doteq 7.2$ km/sec suggest that the penetrating ability of low-density spheres against dual-sheet structures is directly proportional to diameter. The same is true of higher density materials (e.g., aluminum) if the particle mass is less than one gram, but for larger particles the ballistic limit structural thickness required to resist penetration appears to increase at a faster rate than the projectile diameter.

Further investigation of the combined density and size effects noted in the present study appear to be needed. Since the impact velocity has considerable influence on the nature of the debris emanating from the shield, particularly informative would be data at other velocities. In connection with future testing, improvement in the methods of launching large particles at hypervelocity speeds will be advisable.

References

[1] Teng, R. N., "Hypervelocity Impact Damage in Aluminum Targets," Rept. DAC-59816, March 1968, Douglas Aircraft Co., Santa Monica, Calif.

[2] Maiden, C. J., Gehring, J. W., and McMillan, A. R., "Investigation of Fundamental Mechanism of Damage to Thin Targets by Hypervelocity Projectiles," Rept. TR 63-225, Sept. 1963, General Motors Defense Research Labs., Santa Barbara, Calif.

[3] Frost, V. C., Aerospace Corp., private communication, 1968.

[4] Nysmith, C. R., "Penetration Resistance of Double-Sheet Structures at Velocities to 8.8 km/sec," TN D-4568, May 1968, NASA.